REGULAR ARTICLE

The long non-coding RNA KLF3-AS1/miR-10a-3p/ZBTB20 axis improves the degenerative changes in human nucleus pulposus cells

Shijie Chen[1,2] · Quan Zhuang[3] · Pinghuang Li[1] · Jin Zeng[1] · Yi Peng[1] · Zhiyu Ding[1] · Hongqing Cao[1] · Ruping Zheng[4] · Weiguo Wang[1]

Abstract

Excessive apoptosis of intervertebral disc cells, namely nucleus pulposus (NP) cells, results in decreased cell density and extracellular matrix (ECM) catabolism, hence leading to intervertebral disc degeneration (IVDD). As a cell model in the present study, a commercially available human NP cell line was utilized. Long noncoding RNAs and microRNAs may regulate the proliferation or apoptosis of human NP cells, hence exerting a significant influence on the occurrence of IVDD. KLF3-AS1 was discovered to be abnormally downregulated in IVDD tissues. Overexpression of KLF3-AS1 enhanced NP cell viability, prevented cell apoptosis, boosted ECM synthesis, and lowered MMP-13 and ADAMTS4 levels. ZBTB20 and KLF3-AS1 were co-expressed in IVDD; ZBTB20 overexpression had similar effects on NP cells, ECM production, and MMP-13 and ADAMTS4 levels as KLF3-AS1 overexpression. miR-10a-3p may target KLF3-AS1 and ZBTB20 and inhibit the expression of ZBTB20. Inhibition of miR-10a-3p enhanced NP cell viability, reduced apoptosis, and enhanced ECM synthesis. KLF3-AS1 overexpression increased ZBTB20 expression, whereas miR-10a-3p overexpression decreased ZBTB20 expression; miR-10a-3p overexpression reduced the effects of KLF3-AS1 on ZBTB20. Overexpression of miR-10a-3p consistently decreased the effects of KLF3-AS1 overexpression on NP cell survival, apoptosis, and ECM synthesis. In conclusion, KLF3-AS1 overexpression may ameliorate degenerative NP cell alterations through the miR-10a-3p/ZBTB20 axis.

Keywords Intervertebral disc degeneration (IVDD) · Human nucleus pulposus (NP) cells · Long non-coding RNA KLF3-AS1 · miR-10a-3p · ZBTB20

Introduction

Adults may experience a decline in quality of life as a result of intervertebral disc degeneration (IVDD), which causes lower back or upper neck pain and disc herniation (Chen et al. 2009). Multiple variables, including inflammation, matrix degradation, proteoglycan loss in the nucleus pulposus (NP), disorder of the concentric lamellae in the annulus fibrosus (AF), and spinal instability, have been reported to be implicated in IVDD pathogenesis (Grunhagen et al. 2011; Stephan et al. 2011; Huang et al. 2014).

Excessive apoptosis of intervertebral disc cells leads to reduced cell density and extracellular matrix (ECM) catabolism (Park et al. 2001), both of which have crucial implications on IVDD. Additionally, diminished viable cell populations within the NP may also promote IVDD (Buckwalter 1995; Antoniou et al. 1996). It is hypothesized that NP cell–produced type II collagen, aggrecan, and certain ECM components are crucial for maintaining the integrity of intervertebral disc (IVD) (Pockert et al. 2009; Ding et al. 2012). Furthermore, it was previously reported that the upregulation of matrix metalloproteinase (MMP) and aggrecanase expression and activity is implicated within degenerated intervertebral disc-derived cells (Zhang et al. 2008; Gruber et al. 2009; Ding et al. 2012). Aggrecan breakdown results in disc dehydration,

Shijie Chen and Quan Zhuang contribute equally to this study.

✉ Weiguo Wang
csuwwg@csu.edu.cn

1 Department of Orthopaedics, The Third Xiangya Hospital of Central South University, 138 Tongzipo Rd, Changsha, Hunan 410013, China

2 Shanghai Key Laboratory of Regulatory Biology, Institute of Biomedical Sciences and School of Life Sciences, East China Normal University, Shanghai 200241, China

3 Transplantation Center, the Third Xiangya Hospital of Central South University, Hunan 410013, China

4 School of Basic Medical Science, Central South University, Changsha, Hunan 410013, China

subsequently impacting the disc's compression resistance and height (Cabraja et al. 2013). The aggrecanases are metalloproteases that belong to the ADAMTS (a disintegrin and metalloproteinase with thrombospondin motifs) family of extracellular proteases, which contribute to aggrecan degradation (Tian et al. 2013). The expression levels of ADAMTS-4 and ADAMTS-5 showed to be increased within human degenerative disc disease (Hatano et al. 2006). Thus, the loss of NP cells, the subsequent decrease in collagen type II and aggrecan, and the increase in MMPs and ADAMTS are required for disc degeneration.

An increasing amount of evidence suggests that noncoding RNAs, mainly long non-coding RNAs (lncRNAs) and microRNAs (miRNAs), could regulate the proliferation or apoptosis of human NP cells, thus exerting a critical effect on IVDD occurrence (Wang et al. 2011; Liu et al. 2013; Chen et al. 2015, 2017). Recently, Wan et al. (2014) performed a lncRNA-mRNA microarray to detect lncRNA expression levels within human degenerative and normal NP samples. A total of 67 lncRNAs were considerably upregulated and 49 lncRNAs were significantly downregulated, and their fold-changes were all greater than 10. Multiple lncRNAs undergo post-transcriptional processing to yield a variety of short RNAs, such as miRNAs (Rashid et al. 2016). Furthermore, lncRNAs serve as competitive endogenous RNAs or natural miRNA sponges by occupying the common binding regions of miRNAs and thereby sequestering the miRNAs (Chen et al. 2017). The search for the lncRNA-miRNA-mRNA axis implicated in NP cell apoptosis and ECM formation may yield new IVDD treatment targets.

Gene Expression Omnibus dataset GSE70362 for differentially expressed genes in low-grade and high-grade IVDD samples was downloaded and analyzed; KLF3-AS1 was chosen due to its reported function in bone-related disorders. The expression of KLF3-AS1 was then confirmed in tissue samples, and the effects of KLF3-AS1 on the viability and apoptosis of NP cells and ECM formation were investigated. Then, co-expressed mRNAs with KLF3-AS1 were evaluated, and ZBTB20 was chosen. The effects of KLF3-AS1 on the viability and apoptosis of NP cells and the formation of ECM were analyzed. Using an online tool, we examined miRNAs that may target KLF3-AS1 and ZBTB20 and chose miR-10a-3p. The predicted miR-10a-3p binding to KLF3-AS1 and ZBTB20 was validated; the specific effects of miR-10a-3p upon NP cells and the dynamic effects of KLF3-AS1 and miR-10a-3p upon ZBTB20 expression and NP cells were examined. We established a novel lncRNA-miRNA-mRNA axis that modulates NP cell survival, apoptosis, and ECM synthesis.

Materials and methods

Tissue specimen collection

Twelve normal lumbar disc specimens were harvested from the patients with spinal trauma undergoing spinal surgery. The fifteen degenerative specimens were collected from IVDD patients undergoing spinal surgery. All the procedures adhered to the 2013 Declaration of Helsinki and obtained the approval of the Institutional Review Board of The Third Xiangya Hospital of Central South University; informed consent was signed by each patient enrolled.

H&E staining

Tissue samples were fixed in 4% paraformaldehyde, embedded in paraffin, and cut into 4-µm-thick sections. H&E staining was performed for histopathological feature observation (Qin et al. 2019).

Real-time quantitative polymerase chain reaction

The total RNA from target cells or tissues was extracted. The oligo-dT-based transcriptor first-strand cDNA synthesis kit (Roche Diagnostics, Basel, Switzerland) was used to synthesize the cDNA following the manufacturer's instructions. A total of 500 ng total RNA was subsequently added and the product was diluted with RNAse-free H_2O to a final concentration of 5 ng/µl. RT-qPCR detection was performed using a Power SYBR Green PCR master mix (Life Technologies, Carlsbad, California, USA) and ABI Prism 7900HT instrument (Applied Biosystems, Carlsbad, California, USA). The relative expression levels were calculated using the $2^{-\Delta\Delta Ct}$ method and the GAPDH mRNA level was taken as an internal reference.

Cell lineage and cell culture

Human NP cells (Catalog #4800) were obtained from ScienCell (Carlsbad, CA, USA) and maintained in Dulbecco's modified Eagles medium (Invitrogen, Carlsbad, CA, USA) and 10% fetal bovine serum (Invitrogen) supplemented with antibiotics. All the cells were cultured at 37 °C in 5% CO_2 and showed vimentin and fibronectin positive (Fig. S1).

Cell transfection

The overexpression of lncRNA KLF3-AS1 or ZBTB20 was achieved by transfecting KLF3-AS1-overexpressing (KLF3-AS1 OE) or ZBTB20 (ZBTB20 OE) vector to target cells. KLF3-AS1 OE and ZBTB20 OE were constructed based on the pLVX-puro vector (Catalog No. 632164; Takara Bio, Kusatsu, Japan). The overexpression or inhibition of miR-10a-3p was achieved by transfecting agomir-10a-3p or antagomir-10a-3p (GenePharma, Shanghai, China). All the transduction was performed with the help of Lipofectamine™ 3000 Transfection Reagent (Thermo Fisher Scientific, Waltham, MA, USA).

Toluidine blue staining

The NP cells were planted on a glass slide, rinsed with PBS, fixed with paraformaldehyde for 30 min at room temperature, and rinsed with PBS 3 times for 5 min each time. Then stain the NP cells with 1% toluidine blue for 5 min, wash with double-distilled water for 1 min, observe, and take pictures under an inverted phase contrast microscope.

Immunofluorescent staining

NP cells were fixed with 4% paraformaldehyde for 10 min and washed with iced PBS thrice. For antigen retrieval, 100 mM Tris with 5% [W/V] urea (pH 9.5) was used, and cells were permeated with 0.5% Triton X-100 for 10 min. NP cells were subsequently incubated with a PBST of 1% BSA for 30 min for blocking the non-specific binding of the antibodies. NP cells were then incubated with anti-Aggrecan (13880-1-AP, Proteintech, Wuhan, China) or anti-Collagen II (CSB-PA005739ESR2HU, Cusabio, Wuhan, China) at 4 °C overnight. After the incubation, the cells were washed with PBS thrice for 5 min per time. The cells were treated in the dark for 1 h at room temperature with FITC-conjugated secondary antibody (Beyotime, Shanghai, China) (soluble in 1% BSA). The secondary antibody solution was poured and the cells were washed with PBS in the dark thrice, 5 min each time. NP cells were then incubated with DAPI (DNA staining) for 1 min for nucleus staining and then rinsed with PBS. The cover glass was sealed with nail polish and a drop of sealing medium. The results were examined and photographed using a fluorescence microscope (Olympus). Aggrecan or Collagen II fluorescence appeared green, while nuclei fluorescence appeared blue.

CCK-8 for cell viability

The cell viability was detected using a CCK-8 kit (Beyotime). A total of 5×10^3 cells were planted into each well of a 96-well plate. A total of 20 μl of CCK-8 solution was added to each well and incubated with the cells for 2 h at 37 °C. At the end of the incubation, the optical density (OD) value was measured at 450 nm through a microplate reader.

Flow cytometry assay

NP cell apoptosis was measured using an Annexin V-FITC Apoptosis Detection Kit (Beyotime). NP cells were transduced for 48 h, dissociated with 0.25% trypsin without EDTA, and incubated with test solution in the chemical kit according to the manufacturer's instructions. Finally, a flow cytometer was used to evaluate apoptotic NP cells (ACEA Biosciences, U.S.A.).

Immunoblotting

The hypotonic iced buffer was used to lyse target cells. After determining protein concentrations, protein samples were loaded and separated using SDS–PAGE. The blots were subsequently transferred to a PVDF membrane and treated for 24 h at 4 °C with the primary antibodies. The following antibodies were used: anti-Aggrecan (13880-1-AP, Proteintech), anti-Collagen II (CSB-PA005739ES-R2HU, Cusabio), anti-SOX9 (ab185966, Abcam), anti-MMP13 (CSB-PA07029A0Rb, Cusabio), anti-ADAMTS4 (ab185722, Abcam), and anti-ZBTB20 (ab127702, Abcam). The membrane was then treated with an HRP-conjugated secondary antibody (1:1000) at room temperature for 1 h. The enhanced chemiluminescence reagent allowed for the imaging of the proteins.

Immunohistochemical staining (IHC staining)

The tissue sections were fixed in acetone for 10 min − 20 °C, permeabilized with 0.2% triton (Sigma, St. Louis, MO, USA) at room temperature for 10 min, and then incubated with a blocking solution (3.75% BSA/5% goat serum; Zymed, Carlsbad, CA, USA) for 30 min. The samples were subsequently incubated with anti-ZBTB20 (ab127702, Abcam) for 1 h at room temperature. All sections were incubated with the HRP-conjugated poly-anti-rabbit antibody (Boster Biotech, Wuhan, China) for 30 min at 37 ℃. Finally, sections were observed under a microscope after being treated with freshly prepared DAB reagent (Boster Biotech) for 5 min.

Dual-luciferase reporter assay

KLF3-AS1 fragment or ZBTB20 3′-UTR fragment containing conserved miR-10a-3p binding sites were amplified by PCR and subcloned into the psiCHECK™-2 vector (Promega Corporation, Madison, USA) for generating wild-type reporter plasmids, wt-KLF3-AS1, and wt-ZBTB20 3′-UTR. A mutation was introduced

to the predicted miR-10a-3p binding site in KLF3-AS1 or ZBTB20 3′-UTR for generating mutant-type reporter plasmids, mut-ZBTB20 3′-UTR. HEK-293 cells were co-transfected with the aforesaid luciferase vector (200 ng) and either agomiR-10a-3p or antagomiR-10a-3p using Lipofectamine 3000 (Invitrogen). The luciferase activity was then measured 48 h after transfection using a luminometer (Promega, Madison, USA) according to the manufacturer's instructions.

Data processing and statistical analysis

The data of three independent experiments are expressed as means ± SD, and one-way analysis of variance (ANOVA) was used for statistical analysis and Tukey's multiple comparison test or independent sample t-test. The significance level is based on the probability of $P < 0.05$ or $P < 0.01$. SPSS 17.0 statistical software was used for all the analyses.

Results

KLF3-AS1 is downregulated in degenerative intervertebral disc tissues

Firstly, the expression level of KLF3-AS1 was confirmed within degenerative whole IVD tissue samples of Thompson grades I–II, III, IV, and V, according to GSE70362. Figure 1a illustrates that the expression level of KLF3-AS1 was dramatically decreased within high-grade IVDD tissues. Moreover, according to GSE70362, the expression level of KLF3-AS1 was significantly reduced in nucleus pulposus tissues (NP cells) from high-grade degenerative intervertebral disc tissues (Kazezian et al. 2015) (Fig. 1b). The expression of KLF3-AS1 was significantly reduced in the entire blood of IVDD patients compared to that of healthy controls according to GSE124272 (Wang et al. 2019) (Fig. 1c).

The histopathological characteristics of degenerative whole intervertebral disc tissues and normal control tissues were confirmed by H&E staining (Fig. 1d, d'). In addition,
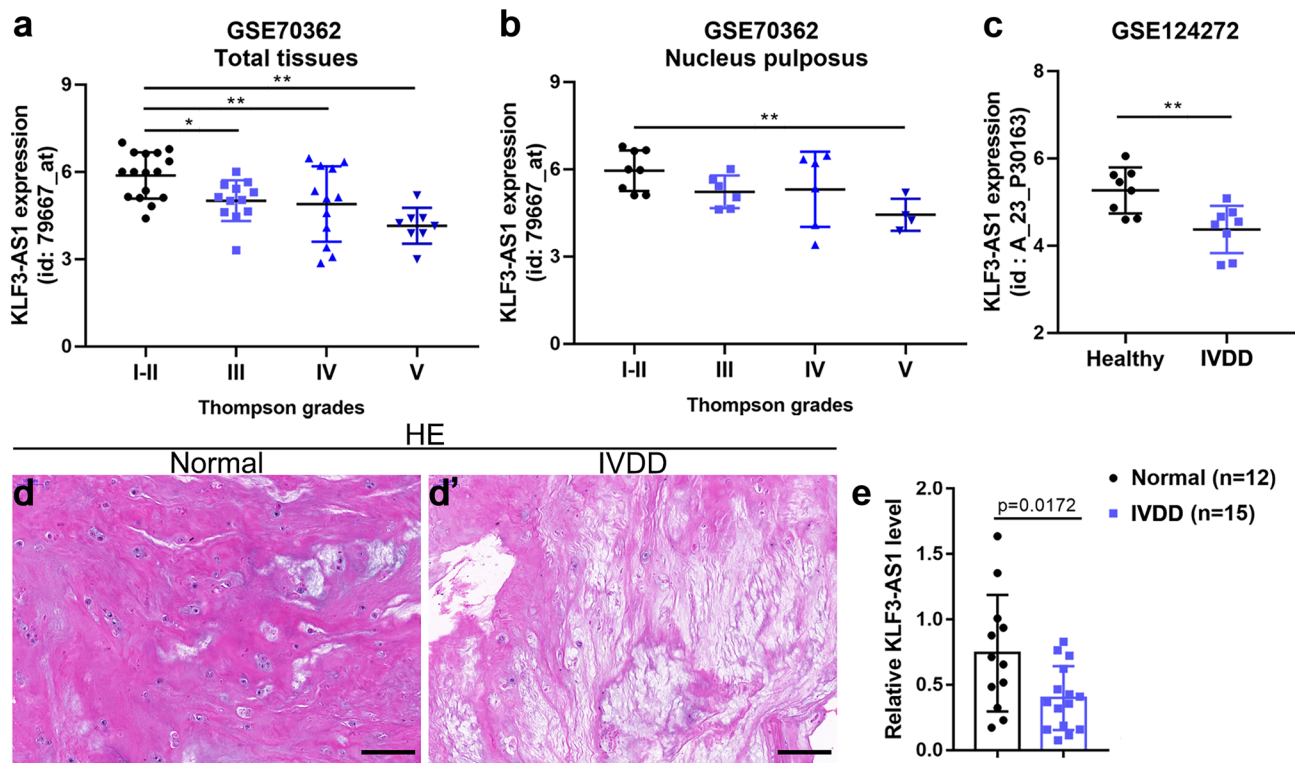

Fig. 1 KLF3-AS1 is downregulated in degenerative intervertebral disc tissues. (**a**) KLF3-AS1 expression in degenerative whole intervertebral disc tissues of Thompson grades I–II, III, IV, and V, according to GSE70362. (**b**) KLF3-AS1 expression in nucleus pulposus tissues from degenerative intervertebral disc tissues of Thompson grades I–II, III, IV, and V, according to GSE70362. (**c**) KLF3-AS1 expression in the whole blood of patients with intervertebral disc degeneration (IVDD) and healthy controls, according to GSE124272. (**d**, **d**') Degenerative whole intervertebral disc tissues and normal control tissues were collected and the histopathological features were confirmed by H&E staining. (**e**) KLF3-AS1 expression was examined in IVDD ($n=15$) and normal control ($n=12$) samples by qRT-PCR. *$P < 0.05$, **$P < 0.01$

the expression level of KLF3-AS1 in IVDD tissues was significantly lower than that in the control group (Fig. 1e).

Specific effects of KLF3-AS1 overexpression on NP cells

Considering the importance of NP cell activities in the etiology of IVDD, we continued to investigate the impact of KLF3-AS1 on NP cell phenotypes. Toluidine blue staining revealed chondrocyte-like characteristics of NP cells (Fig. 2a), while immunofluorescent (IF) staining revealed amounts of Aggrecan and Collagen II in NP cells (Fig. 2b, b'). Transduction of a KLF3-AS1-overexpressing vector into NP cells led to KLF3-AS1 overexpression (KLF3-AS1 OE). The overexpression of KLF3-AS1 was confirmed by qRT-PCR (Fig. 2c). KLF3-AS1 overexpression significantly promoted NP cell proliferation and inhibited cell apoptosis (Fig. 2d–e''). As for ECM deposition, KLF3-AS1 overexpression increased Aggrecan, Collagen II, and Sox-9 proteins while decreasing MMP-13 and ADAMTS4 proteins (Fig. 2f, f').

ZBTB20 is positively correlated with KLF3-AS1

To select the KLF3-AS1 expression-related genes, Pearson's correlation coefficient was used to analyze the expression correlation based on GSE70362 and GSE124272 ($|r| > 0.5$, $p < 0.05$). Six gene (DDHD2, LINC00342, ZBTB20, SUN1, NR3C1, and ZFP90) expressions were positively correlated with KLF3-AS1 expression, and 3 gene (NGRN, C12orf49 and TFPI) expression were negatively correlated with KLF3-AS1 expression in both GSE datasets. ZBTB20 has the highest correlation coefficient r value. According to GSE124272, the expression level of ZBTB20 in IVDD patients' whole blood was significantly lower than that of healthy controls (Fig. 3a). Also, according to GSE124272, ZBTB20 expression in tissue samples was favorably linked with KLF3-AS1 expression (Fig. 3b). IHC staining and qRT-PCR demonstrated that ZBTB20 protein and mRNA levels were significantly lower in IVDD tissues than in control group tissues (Fig. 3c, d). ZBTB20 was positively associated with KLF3-AS1 in collected tissue samples (Fig. 3e).

Specific effects of ZBTB20 overexpression on NP cells

After establishing the overexpression of ZBTB20 and its favorable connection with KLF3-AS1, the particular effects of ZBTB20 on NP cells were studied. KLF3-AS1 overexpression within NP cells dramatically boosted ZBTB20 protein levels (Fig. 4a, a'). NP cells were then transduced with a ZBTB20-overexpressing vector to produce ZBTB20 overexpression (ZBTB20 OE). Immunoblot

analyses verified the overexpression of ZBTB20 (Fig. 4b, b'). Similar to KLF3-AS1 overexpression, ZBTB20 overexpression increased NP cell viability and suppressed apoptosis (Fig. 4c–d''). In addition, the overexpression of ZBTB20 increased Aggrecan, Collagen II, and Sox-9 proteins while decreasing MMP-13 and ADAMTS4 proteins during ECM deposition (Fig. 4e, e').

miR-10a-3p directly targets KLF3-AS1 and ZBTB20

Since microRNA could mediate the crosstalk between lncRNA and mRNA, we searched for microRNAs that could simultaneously target KLF3-AS1 and ZBTB20. Online resources and databases converged in miR-10a-3p and miR-5584p (Fig. 5a). In order to select one miRNA, we compared the expression levels of miR-10a-3p and miR-5584-3p in IVDD and normal tissue samples; Fig. 5b demonstrates that the expression level of miR-10a-3p was considerably higher in IVDD tissue samples than in control group samples (Fig. 5b, b').

agomir-10a-3p or antagomir-10a-3p was transduced into NP cells to induce miR-10a-3p expression, and qRT-PCR was used to demonstrate miR-10a-3p overexpression or inhibition (Fig. 5c). Overexpression of miR-10a-3p lowered in NP cells, but inhibition of miR-10a-3p increased ZBTB20 protein levels (Fig. 5d, d'). To confirm the proposed binding of miR-10a-3p to KLF3-AS1 and ZBTB20, we produced wild-type and mutant-type KLF3-AS1 and ZBTB20 luciferase reporter vectors, as well as co-transfected reporter vectors in NP cells with agomir-10a-3p/antagomir-10a-3p. When co-transfected with wild-type reporter vectors (wt-KLF3-AS1/wt-ZBTB20), miR-10a-3p overexpression inhibited, whereas miR-10a-3p inhibition enhanced the luciferase activity of the reporter vectors, when co-transfected with mutant-type reporter vectors (mut-KLF3-AS1/mut-ZBTB20), miR-10a-3p overexpression or inhibition failed to alter the luciferase activity (Fig. 5e, f).

Specific effects of miR-10a-3p on NP cells

Since miR-10a-3p targets ZBTB20, it is speculated that it also plays a role in NP cell phenotypes. Target cells are transduced with antagomir-NC or antagomir-10a-3p and evaluated cell phenotypes to verify the hypothesis. Figure 6a–b'' demonstrated that inhibiting miR-10a-3p increased NP cell viability while inhibiting cell death. MiR-10a-3p suppression increased Aggrecan, Collagen II, and Sox-9 proteins but decreased MMP-13 and ADAMTS4 proteins during ECM deposition (Fig. 6c, c').
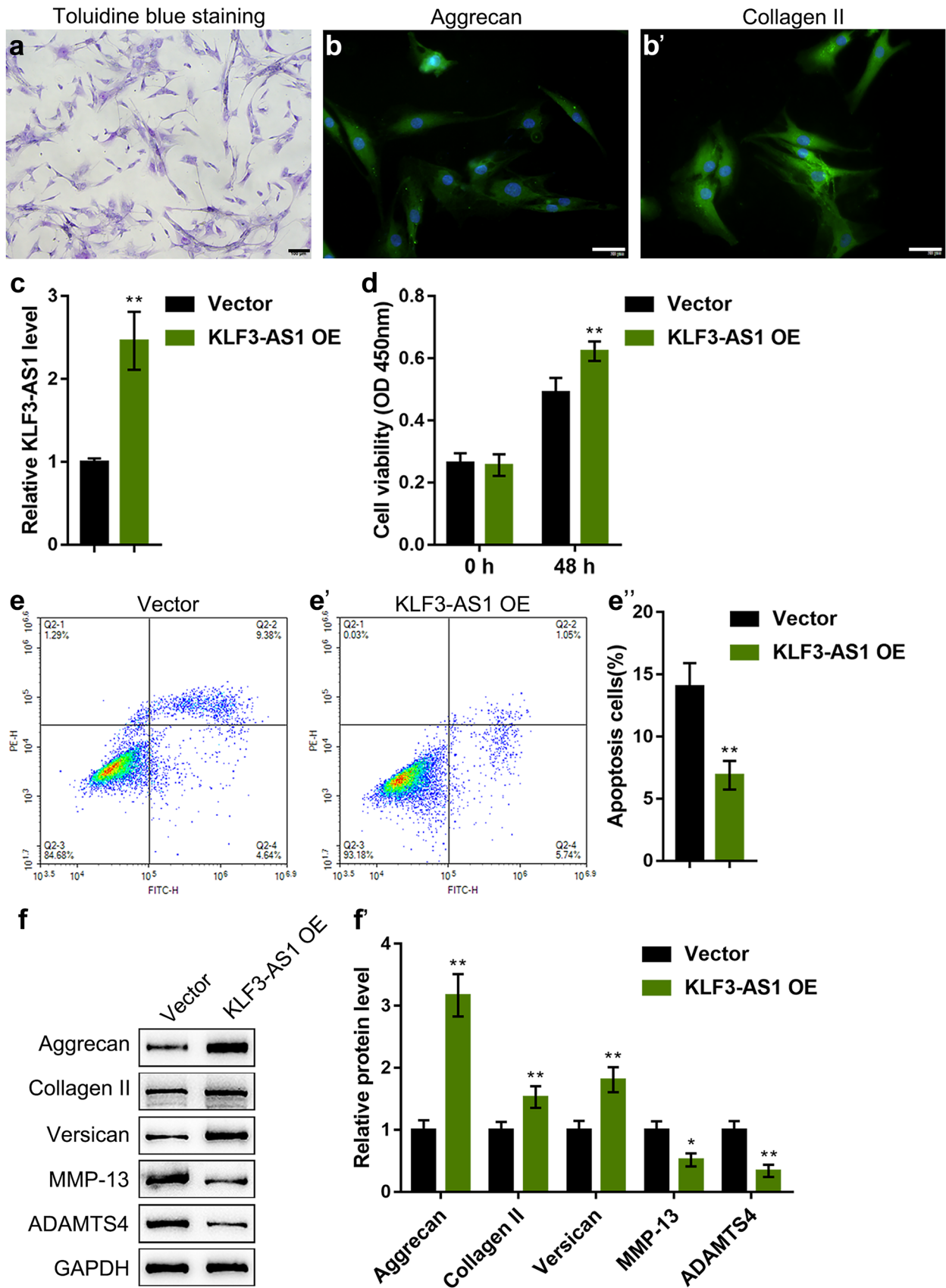
Toluidine blue staining	Aggrecan	Collagen II

◄**Fig. 2** Specific effects of KLF3-AS1 overexpression on NP cells. (**a**) NP cells were identified using Toluidine blue staining for chondrocyte-like features. (**b**, **b'**) NP cells were identified using immunofluorescent (IF) staining for Aggrecan and Collagen II levels. (**c**) KLF3-AS1 overexpression was achieved in NP cells by transducing KLF3-AS1-overexpressing vector (KLF3-AS1 OE). The overexpression of KLF3-AS1 was confirmed by qRT-PCR. Then, NP cells were transduced with KLF3-AS1 OE or negative control (vector) and examined for cell viability by CCK-8 assay (**d**); cell apoptosis by flow cytometry (**e–e''**); the protein levels of Aggrecan, Collagen II, Sox-9, MMP-13, and ADAMTS4 by immunoblotting (**f**, **f'**). *$P < 0.05$, **$P < 0.01$

Dynamic effects of KLF3-AS1 and miR-10a-3p on NP cells

Finally, it was examined if KLF3-AS1 might offset the effects of miR-10a-3p on ZBTB20 expression. ZBTB20 protein levels were measured in target cells co-transduced with KLF3-AS1 OE and agomir-10a-3p. KLF3-AS1 overexpression increased the protein levels of ZBTB20, while miR-10a-3p overexpression decreased them; the effects

Fig. 3 ZBTB20 is positively correlated with KLF3-AS1. (**a**) ZBTB20 expression in the whole blood of patients with intervertebral disc degeneration (IVDD) and healthy controls, according to GSE124272. (**b**) The correlation between ZBTB20 and KLF3-AS1 expression in tissue samples, according to GSE124272, analyzed by Pearson's correlation analysis. (**c**, **c'**) ZBTB20 levels in tissue samples were examined using Immunohistochemical (IHC) staining. (**d**) ZBTB20 mRNA levels in tissue samples were examined using qRT-PCR. (**e**) The correlation between ZBTB20 and KLF3-AS1 expression in tissue samples analyzed by Pearson's correlation analysis. *$P < 0.05$
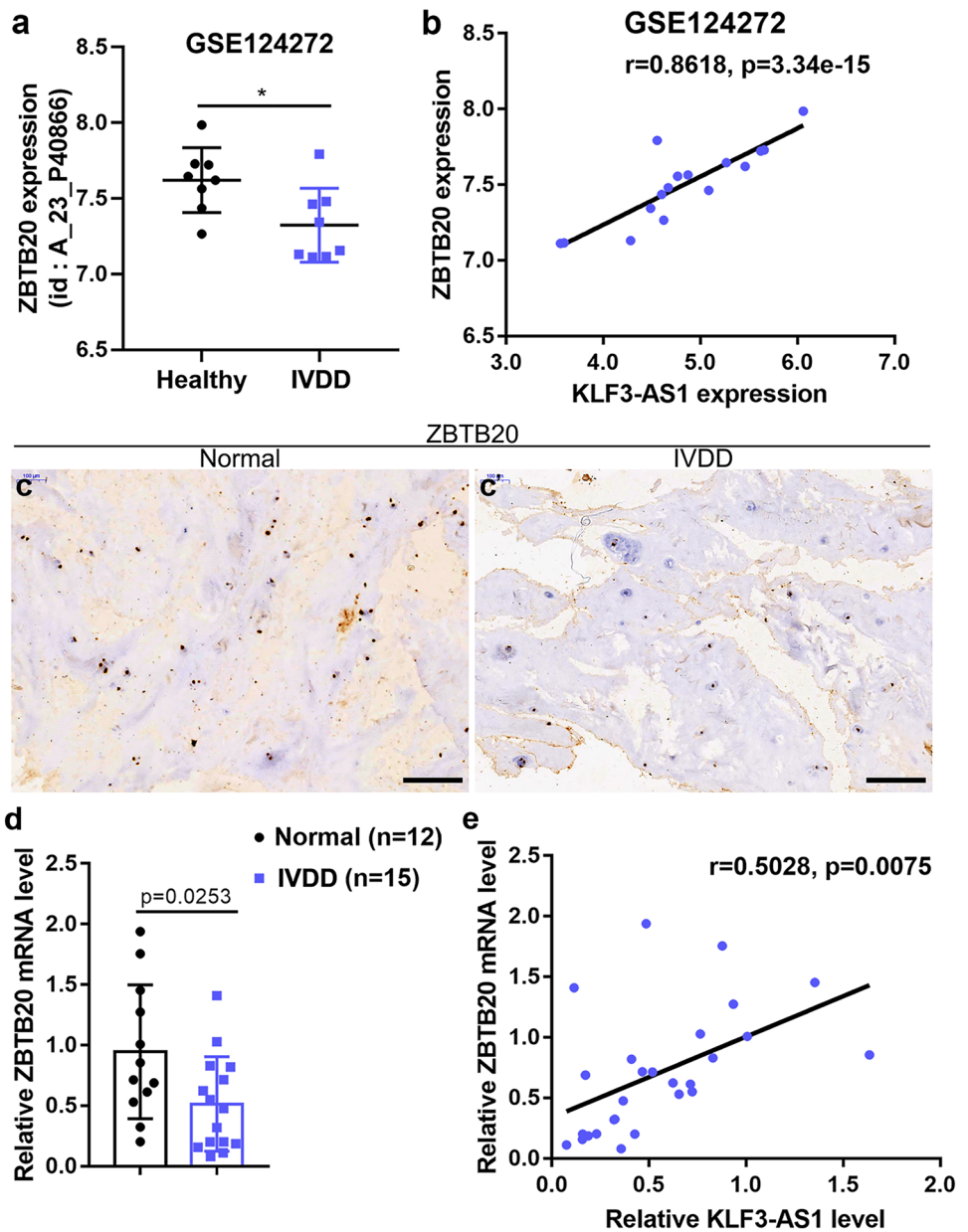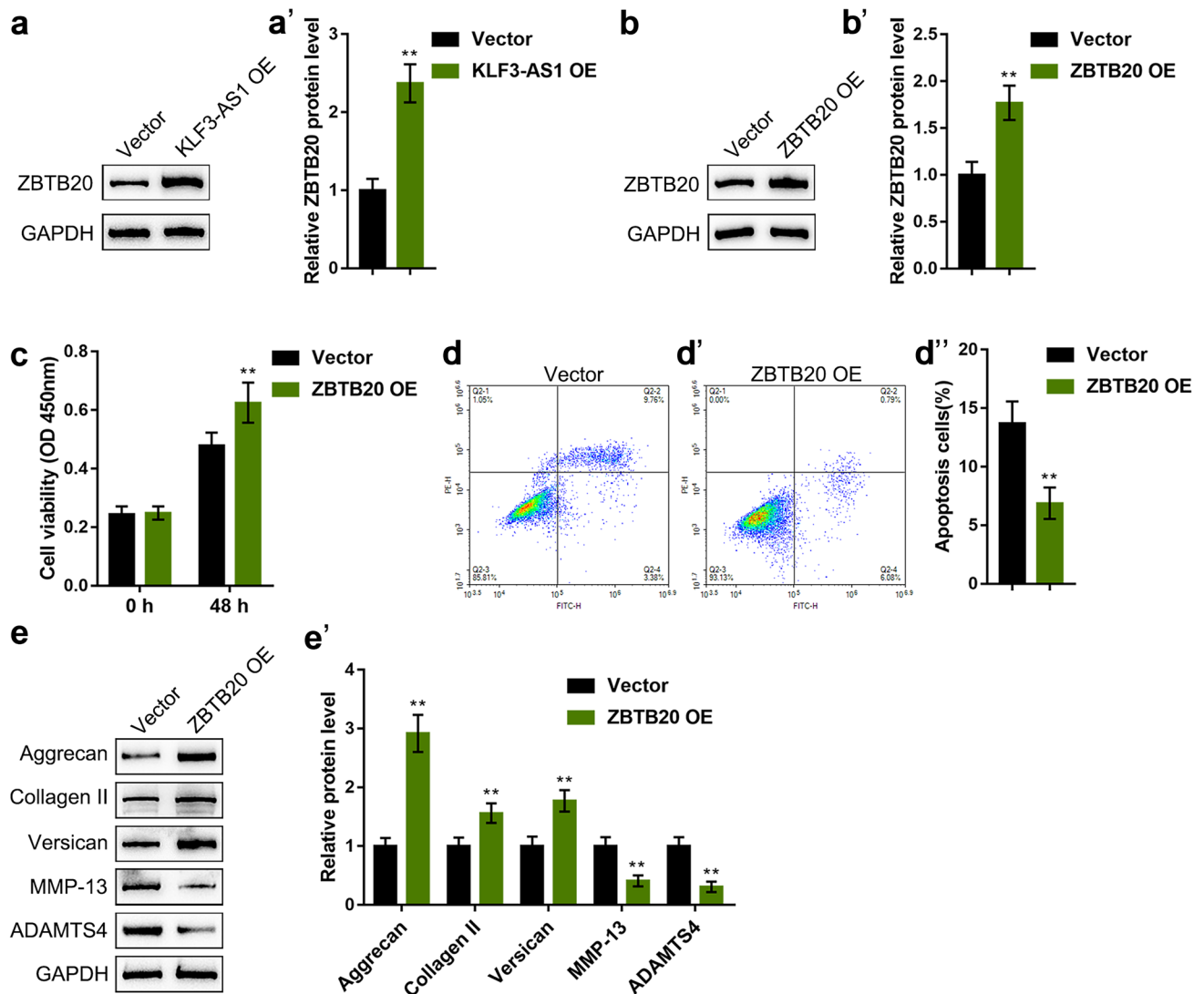
Fig. 4 Specific effects of ZBTB20 overexpression on NP cells. (**a**, **a'**) NP cells were transduced with KLF3-AS1 OE and examined for the protein levels of ZBTB20 by immunoblotting. (**b**, **b'**) ZBTB20 overexpression was achieved in NP cells by transducing ZBTB20-overexpressing vector (ZBTB20 OE). The overexpression of ZBTB20 was confirmed by immunoblotting. Then, NP cells were transduced with ZBTB20 OE or negative control (vector) and examined for cell viability by CCK-8 assay (**c**); cell apoptosis by flow cytometry (**d**–**d''**); the protein levels of Aggrecan, Collagen II, Sox-9, MMP-13, and ADAMTS4 by Immunoblotting (**e**, **e'**). **$P < 0.01$

of KLF3-AS1 overexpression on ZBTB20 were partially moderated by miR-10a-3p overexpression. In the meantime, Fig. 7a, a' demonstrates that KLF3-AS1 overexpression increased Aggrecan, Collagen II, and Sox-9 levels and decreased MMP-13 and ADAMTS4 levels, while miR-10a-3p overexpression had the opposite effect on these proteins; similarly, the effects of KLF3-AS1 overexpression on these proteins were partially attenuated by miR-10a-3p overexpression. Overexpression of miR-10a-3p had the reverse impact of that of KLF3-AS1; the effects of KLF3-AS1 overexpression on NP cell phenotypes were partially mitigated by miR-10a-3p overexpression (Fig. 7b–c'''').

Discussion

This study investigates the roles and mechanisms of the KLF3-AS1/miR-10a-3p/ZBTB20 axis in NP cell morphologies and IVDD progression, as hyper apoptosis of NP cells could lead to decreased cell density and ECM degradation, hence contributing to the development of IVDD. KLF3-AS1 was shown to be abnormally downregulated inside IVDD tissues. Overexpression of KLF3-AS1 enhanced NP cell viability, prevented cell apoptosis, boosted ECM synthesis, and lowered MMP-13 and ADAMTS4 levels. ZBTB20 and KLF3-AS1 were co-expressed in IVDD; ZBTB20
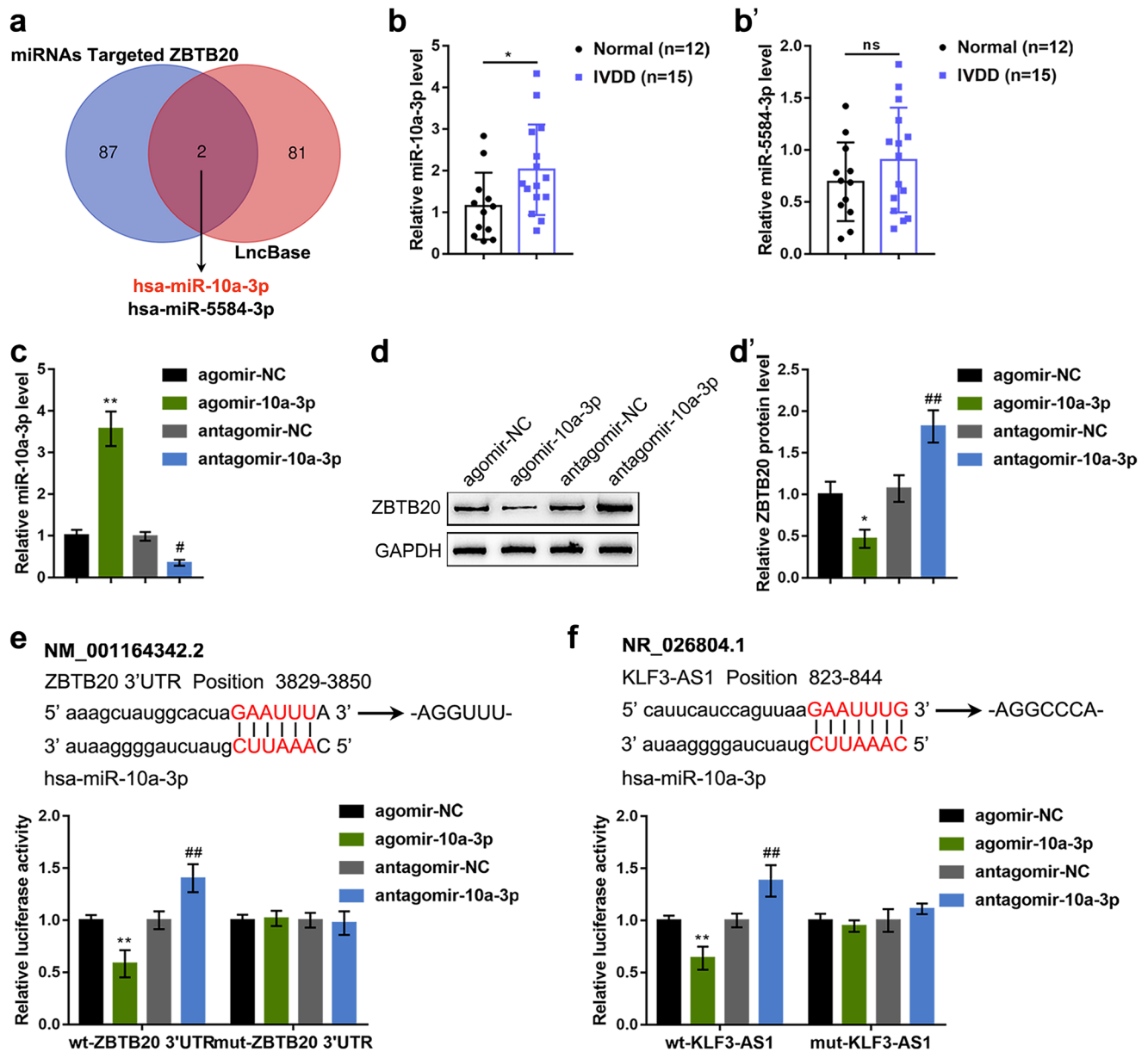
Fig. 5 miR-10a-3p directly targets KLF3-AS1 and ZBTB20. (**a**) Online tools and database were used to screen for miRNAs that might target KLF3-AS1 and ZBTB20 simultaneously; 2 miRNAs were obtained. (**b**, **b'**) The expression levels of miR-10a-3p and miR-5584-3p in IVDD and normal tissues were examined using qRT-PCR. (**c**) miR-10a-3p expression was achieved in NP cells by transducing agomir-10a-3p or antagomir-10a-3p. The overexpression or inhibition of miR-10a-3p was confirmed by qRT-PCR. (**d, d'**) NP cells were transduced with agomir-10a-3p or antagomir-10a-3p and examined for the protein levels of ZBTB20 by Immunoblotting. (**e–f**) Wild- and mutant-type KLF3-AS1 and ZBTB20 luciferase reporter vectors were constructed and co-transfected in NP cells with agomir-10a-3p or antagomir-10a-3p; the luciferase activity was determined. $*P < 0.05$, $**P < 0.01$, $\#P < 0.05$, $\#\#P < 0.01$

overexpression had similar effects on NP cells, ECM synthesis, and MMP-13 and ADAMTS4 levels as KLF3-AS1 overexpression. miR-10a-3p may target KLF3-AS1 and ZBTB20 and suppress the expression of ZBTB20. Inhibition of miR-10a-3p enhanced NP cell viability, reduced cell death, and enhanced ECM synthesis. KLF3-AS1 overexpression increased ZBTB20 expression, whereas miR-10a-3p overexpression decreased ZBTB20 expression;

miR-10a-3p overexpression reduced the effects of KLF3-AS1 on ZBTB20. Overexpression of miR-10a-3p consistently decreased the effects of KLF3-AS1 overexpression on NP cell survival, apoptosis, and ECM synthesis.

KLF3-AS1 is an MSC-Exos-derived lncRNA (Ensembl: ENST00000440181) reported in ExoCarta (http://www.exocarta.org). It has been shown that KLF3-AS1 exerts a tumor-suppressive effect on esophageal squamous cell carcinoma
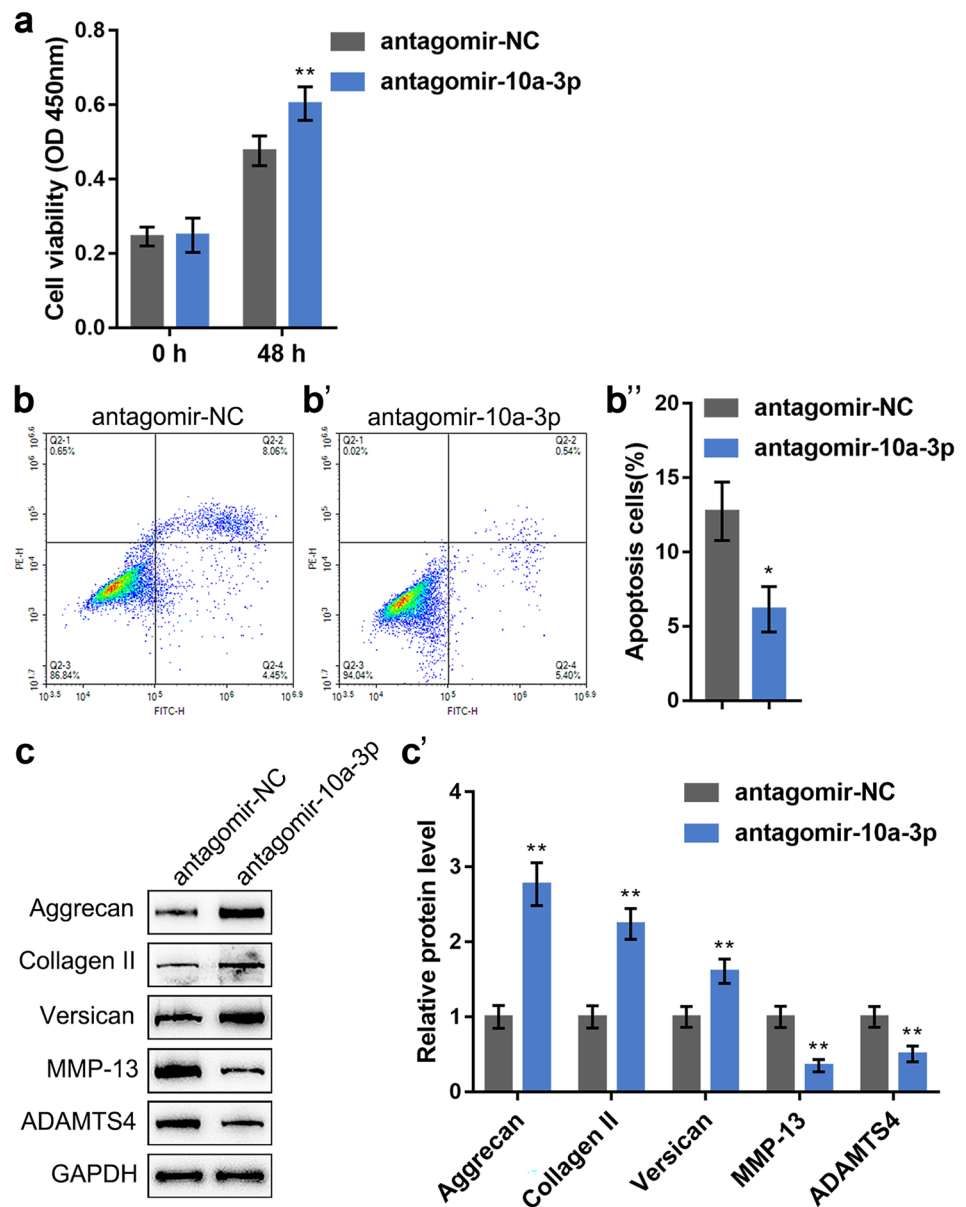
by decreasing the inhibitory effect generated by miR-185-5p on KLF3 to inhibit the tumor cells' ability to invade and migrate (Liu et al. 2020). Overexpression of the exosomal lncRNA KLF3-AS1 from MSCs lowered cell apoptosis and pyroptosis, as well as the extent of the myocardial infarction, and halted the progression of myocardial infarction in cardiomyocytes exposed to hypoxia (Mao et al. 2019). Reportedly, in osteoarthritis, exosomal KLF3-AS1 could promote chondrocyte proliferation and inhibit apoptosis (Liu et al. 2018a, b), which is at odds with its role in esophageal squamous cell cancer. In the current investigation, abnormal downregulation of KLF3-AS1 was detected in IVDD tissue samples, indicating a potential role in the etiology of IVDD.

The acceleration of NP cell apoptosis and senescence would produce IVDD, leading to a number of detrimental effects,

including cell cycle arrest, limited cell viability, increased pro-inflammatory activity, and decreased expression of matrix macromolecules (Feng et al. 2017; Xie et al. 2018). The ECM produced by NP cells is predominantly composed of proteoglycan and collagen II, which play a crucial role in the pathophysiology of IVDD (Vergroesen et al. 2015). In IVDD, the breakdown of type II collagen and proteoglycan (mostly aggrecan) is mediated by MMP3 and MMP13, which are elevated within degenerated NP cells (Wang et al. 2017a, b), and the loss of the balance between ECM deposition and degradation would result in the mitigation of intervertebral disc structural integrity, thereby promoting IVDD development (Kepler et al. 2013). In the current study, KLF3-AS1 overexpression enhanced NP cell viability, prevented cell apoptosis, elevated Aggrecan and Collagen II levels, and lowered MMP-13 and
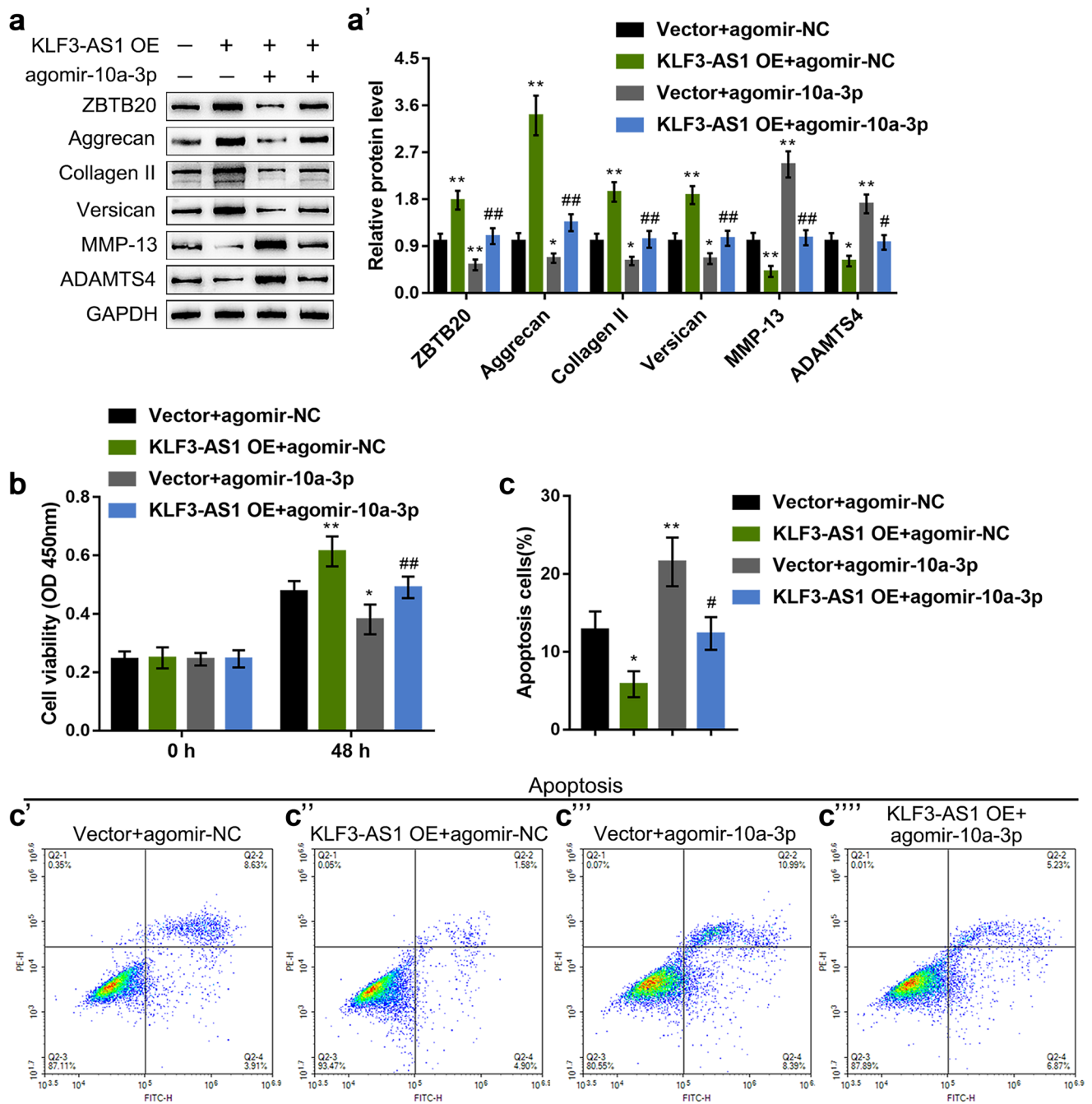
Fig. 7 Dynamic effects of KLF3-AS1 and miR-10a-3p on NP cells. Target cells were co-transduced with KLF-AS1 OE and agomir-10a-3p and examined for the protein levels of ZBTB20, Aggrecan, Collagen II, Sox-9, MMP-13, and ADAMTS4 by immunoblotting (**a**, **a**'); cell via-bility by CCK-8 assay (**b**); cell apoptosis by flow cytometry (**c**–**c**''''). *$P < 0.05$, **$P < 0.01$, compared with the control group; #$P < 0.05$, ##$P < 0.01$, compared with the vector + agomir-10a-3p group

ADAMTS4 levels, indicating that KLF3-AS1 could improve degenerative alterations in NP cells.

To further explore the molecular mechanism behind KLF3-AS1's role in regulating the phenotypes of NP cells, we discovered that ZBTB20 was co-expressed with KLF3-AS1 and that miR-10a-3p could target both KLF3-AS1

and ZBTB20. In other words, miR-10a-3p targets ZBTB20 and suppresses ZBTB20 expression, but KLF3-AS1 can counteract miR-10a-3p-mediated suppression of ZBTB20. Using chondrocyte-specific Zbtb20 knockout mice, Zhou et al. (2015) found that the absence of chondrocyte Zbtb20 delays endochondral ossification and postnatal growth.

MiR-10a-3p has been linked to the effects of Kaempferol on BMSC osteogenic differentiation and osteoporosis reduction (Liu et al. 2021). In this study, ZBTB20 overexpression or miR-10a-3p inhibition exerted similar effects on NP cells as KLF3-AS1 overexpression; notably, miR-10a-3p overexpression partially attenuated the roles of KLF3-AS1 overexpression in the viability and apoptosis of NP cells, and the protein levels of aggrecan, type II collagen, MMP-13, and ADAMTS4.

These data suggest that KLF3-AS1 overexpression may ameliorate the degenerative alterations in NP cells, presumably via the miR-10-3p/ZBTB20 axis. Regarding the limitations of this investigation, no animal models were utilized to examine the in vivo effects of the KLF3-AS1/miR-10a-3p/ZBTB20 axis. Prior to the clinical application of the axis, animal testing would be required.

Declarations

Consent for publication All procedures were approved by the Institutional Review Board of The Third Xiangya Hospital of Central South University.

Informed consent The informed consent was signed by each patient enrolled in The Third Xiangya Hospital of Central South University.

Ethical approval Not applicable.

Conflict of interest The authors declare no competing interests.

References

Antoniou J, Steffen T, Nelson F, Winterbottom N, Hollander AP, Poole RA, Aebi M, Alini M (1996) The human lumbar intervertebral disc: evidence for changes in the biosynthesis and denaturation of the extracellular matrix with growth, maturation, ageing, and degeneration. J Clin Invest 98(4):996–1003

Buckwalter JA (1995) Aging and degeneration of the human intervertebral disc. Spine (Phila Pa 1976) 20(11):1307–1314

Cabraja M, Endres M, Abbushi A, Zenclussen M, Blechschmidt C, Lemke AJ, Kroppenstedt S, Kaps C, Woiciechowsky C (2013) Effect of degeneration on gene expression of chondrogenic and inflammatory marker genes of intervertebral disc cells: a preliminary study. J Neurosurg Sci 57(4):307–316

Chen WH, Liu HY, Lo WC, Wu SC, Chi CH, Chang HY, Hsiao SH, Wu CH, Chiu WT, Chen BJ, Deng WP (2009) Intervertebral disc regeneration in an ex vivo culture system using mesenchymal stem cells and platelet-rich plasma. Biomaterials 30(29):5523–5533

Chen WK, Yu XH, Yang W, Wang C, He WS, Yan YG, Zhang J, Wang WJ (2017) lncRNAs: novel players in intervertebral disc degeneration and osteoarthritis. Cell Prolif 50(1):e12313

Chen Y, Ni H, Zhao Y, Chen K, Li M, Li C, Zhu X, Fu Q (2015) Potential role of lncRNAs in contributing to pathogenesis of intervertebral disc degeneration based on microarray data. Med Sci Monit 21:3449–3458

Ding F, Shao ZW, Yang SH, Wu Q, Gao F, Xiong LM (2012) Role of mitochondrial pathway in compression-induced apoptosis of nucleus pulposus cells. Apoptosis 17(6):579–590

Feng C, Zhang Y, Yang M, Lan M, Liu H, Huang B, Zhou Y (2017) Oxygen-sensing Nox4 generates genotoxic ROS to induce premature senescence of nucleus pulposus cells through MAPK and NF-kappaB pathways. Oxid Med Cell Longev 2017:7426458

Gruber HE, Ingram JA, Hoelscher GL, Zinchenko N, Norton HJ, Hanley EN Jr (2009) Matrix metalloproteinase 28, a novel matrix metalloproteinase, is constitutively expressed in human intervertebral disc tissue and is present in matrix of more degenerated discs. Arthritis Res Ther 11(6):R184

Grunhagen T, Shirazi-Adl A, Fairbank JC, Urban JP (2011) Intervertebral disk nutrition: a review of factors influencing concentrations of nutrients and metabolites. Orthop Clin North Am 42(4):465–477, vii

Hatano E, Fujita T, Ueda Y, Okuda T, Katsuda S, Okada Y, Matsumoto T (2006) Expression of ADAMTS-4 (aggrecanase-1) and possible involvement in regression of lumbar disc herniation. Spine (Phila Pa 1976) 31(13):1426–1432

Huang YC, Urban JP, Luk KD (2014) Intervertebral disc regeneration: do nutrients lead the way? Nat Rev Rheumatol 10(9):561–566

Kazezian Z, Gawri R, Haglund L, Ouellet J, Mwale F, Tarrant F, O'Gaora P, Pandit A, Alini M, Grad S (2015) Gene expression profiling identifies interferon signalling molecules and IGFBP3 in human degenerative annulus fibrosus. Sci Rep 5:15662

Kepler CK, Ponnappan RK, Tannoury CA, Risbud MV, Anderson DG (2013) The molecular basis of intervertebral disc degeneration. Spine J 13(3):318–330

Liu G, Cao P, Chen H, Yuan W, Wang J, Tang X (2013) MiR-27a regulates apoptosis in nucleus pulposus cells by targeting PI3K. PLoS ONE 8(9):e75251

Liu H, Yi X, Tu S, Cheng C, Luo J (2021) Kaempferol promotes BMSC osteogenic differentiation and improves osteoporosis by downregulating miR-10a-3p and upregulating CXCL12. Mol Cell Endocrinol 520:111074

Liu JQ, Deng M, Xue NN, Li TX, Guo YX, Gao L, Zhao D, Fan RT (2020) lncRNA KLF3-AS1 suppresses cell migration and invasion in ESCC by impairing miR-185-5p-targeted KLF3 inhibition. Mol Ther Nucleic Acids 20:231–241

Liu Y, Lin L, Zou R, Wen C, Wang Z, Lin F (2018a) MSC-derived exosomes promote proliferation and inhibit apoptosis of chondrocytes via lncRNA-KLF3-AS1/miR-206/GIT1 axis in osteoarthritis. Cell Cycle 17(21–22):2411–2422

Liu Y, Zou R, Wang Z, Wen C, Zhang F, Lin F (2018b) Exosomal KLF3-AS1 from hMSCs promoted cartilage repair and chondrocyte proliferation in osteoarthritis. Biochem J 475(22):3629–3638

Mao Q, Liang XL, Zhang CL, Pang YH, Lu YX (2019) LncRNA KLF3-AS1 in human mesenchymal stem cell-derived exosomes ameliorates pyroptosis of cardiomyocytes and myocardial infarction through miR-138-5p/Sirt1 axis. Stem Cell Res Ther 10(1):393

Park JB, Kim KW, Han CW, Chang H (2001) Expression of Fas receptor on disc cells in herniated lumbar disc tissue. Spine (Phila Pa 1976) 26(2):142–146

Pockert AJ, Richardson SM, Le Maitre CL, Lyon M, Deakin JA, Buttle DJ, Freemont AJ, Hoyland JA (2009) Modified expression of the ADAMTS enzymes and tissue inhibitor of metalloproteinases 3 during human intervertebral disc degeneration. Arthritis Rheum 60(2):482–491

Qin D, Zhang H, Zhang H, Sun T, Zhao H, Lee WH (2019) Anti-osteoporosis effects of osteoking via reducing reactive oxygen species. J Ethnopharmacol 244:112045

Rashid F, Shah A, Shan G (2016) Long non-coding RNAs in the cytoplasm. Genom Proteom Bioinform 14(2):73–80

Stephan S, Johnson WE, Roberts S (2011) The influence of nutrient supply and cell density on the growth and survival of intervertebral disc cells in 3D culture. Eur Cell Mater 22:97–108

Tian Y, Yuan W, Fujita N, Wang J, Wang H, Shapiro IM, Risbud MV (2013) Inflammatory cytokines associated with degenerative disc disease control aggrecanase-1 (ADAMTS-4) expression in nucleus pulposus cells through MAPK and NF-kappaB. Am J Pathol 182(6):2310–2321

Vergroesen PP, Kingma I, Emanuel KS, Hoogendoorn RJ, Welting TJ, van Royen BJ, van Dieen JH, Smit TH (2015) Mechanics and biology in intervertebral disc degeneration: a vicious circle. Osteoarthr Cartil 23(7):1057–1070

Wan ZY, Song F, Sun Z, Chen YF, Zhang WL, Samartzis D, Ma CJ, Che L, Liu X, Ali MA, Wang HQ, Luo ZJ (2014) Aberrantly expressed long noncoding RNAs in human intervertebral disc degeneration: a microarray related study. Arthritis Res Ther 16(5):465

Wang C, Zhang ZZ, Yang W, Ouyang ZH, Xue JB, Li XL, Zhang J, Chen WK, Yan YG, Wang WJ (2017a) MiR-210 facilitates ECM degradation by suppressing autophagy via silencing of ATG7 in human degenerated NP cells. Biomed Pharmacother 93:470–479

Wang HQ, Yu XD, Liu ZH, Cheng X, Samartzis D, Jia LT, Wu SX, Huang J, Chen J, Luo ZJ (2011) Deregulated miR-155 promotes Fas-mediated apoptosis in human intervertebral disc degeneration by targeting FADD and caspase-3. J Pathol 225(2):232–242

Wang K, Liu W, Song Y, Wu X, Zhang Y, Li S, Gao Y, Tu J, Liu Y, Yang C (2017b) The role of angiopoietin-2 in nucleus pulposus cells during human intervertebral disc degeneration. Lab Invest 97(8):971–982

Wang Y, Dai G, Li L, Liu L, Jiang L, Li S, Liao S, Wang F, Du W, Li Y (2019) Transcriptome signatures reveal candidate key genes in the whole blood of patients with lumbar disc prolapse. Exp Ther Med 18(6):4591–4602

Xie J, Li B, Zhang P, Wang L, Lu H, Song X (2018) Osteogenic protein-1 attenuates the inflammatory cytokine-induced NP cell senescence through regulating the ROS/NF-kappaB pathway. Biomed Pharmacother 99:431–437

Zhang Q, Hui W, Litherland GJ, Barter MJ, Davidson R, Darrah C, Donell ST, Clark IM, Cawston TE, Robinson JH, Rowan AD, Young DA (2008) Differential Toll-like receptor-dependent collagenase expression in chondrocytes. Ann Rheum Dis 67(11):1633–1641

Zhou G, Jiang X, Zhang H, Lu Y, Liu A, Ma X, Yang G, Yang R, Shen H, Zheng J, Hu Y, Yang X, Zhang WJ, Xie Z (2015) Zbtb20 regulates the terminal differentiation of hypertrophic chondrocytes via repression of Sox9. Development 142(2):385–393